

Alkyne Insertion into the Ru–C Bond of a Four-Membered Metallacycle. Insertion Rate and Reaction Pathway

Kaushik Ghosh, Swarup Chattopadhyay, Sujay Pattanayak, and Animesh Chakravorty*

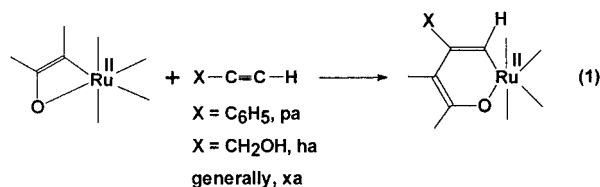
Department of Inorganic Chemistry, Indian Association for the Cultivation of Science, Calcutta 700032, India

Received July 28, 2000

The insertion of $\text{HOCH}_2\text{C}\equiv\text{CH}$ (ha) into the Ru–C bond of $\text{Ru}^{\text{II}}(\text{RL}^1)(\text{PPh}_3)_2(\text{CO})\text{Cl}$, **1**, has afforded $\text{Ru}^{\text{II}}(\text{RL}^3)(\text{PPh}_3)_2(\text{CO})\text{Cl}$, **3**, which has been structurally characterized. Insertion rates in CH_2Cl_2 –MeOH for ha as well as for $\text{PhC}\equiv\text{CH}$ (pa), which inserts similarly into **1** affording $\text{Ru}^{\text{II}}(\text{RL}^2)(\text{PPh}_3)_2(\text{CO})\text{Cl}$, **2**, are proportional to the product of the concentrations of alkyne and methanol. The insertion rate of ha is nearly 5 times faster than that of pa, and for a given alkyne the rate increases as R becomes more electron-withdrawing ($\text{OMe} < \text{Me} < \text{Cl}$). A reaction model implicating the adduct $\mathbf{1}\cdot\text{MeOH}$, which binds and activates the alkyne via displacement of MeOH, is proposed.

Introduction

A few instances of insertion of alkynes into the Ru–C σ -bond have been documented in the literature,^{1–6} but rarely have mechanistic proposals been authenticated by rate studies.⁶ The concern of the present work is the two-carbon metallacycle expansion via insertion of alkynes generally abbreviated as xa, eq 1. The reaction



was recently authenticated by us via isolation and structure determination of the expanded cycle in the case of phenylacetylene, pa (as well as unsubstituted acetylene).¹

Further scrutiny has revealed that the reaction is suitable for facile rate determination by spectrophotometric methods in the cases of pa and hydroxymethylacetylene, ha. This has provided an opportunity for probing the reaction pathway. Rates have been measured in CH_2Cl_2 –MeOH mixtures, revealing that the four-membered metallacycle itself is *not* reactive but its methanol adduct present in equilibrium *is*. The observed rate law has been rationalized on this basis, and a

mechanistic model is proposed. The substituents in the alkyne and the reactive metallacycle have notable effects on reaction rates. The insertion of hydroxymethylacetylene, ha according to eq 1, is being reported here for the first time, necessitating product characterization, which forms a part of the present work.

Results and Discussion

Substrates and Products. The concerned metallacycles, their abbreviations, and numberings are set out in Figure 1. Three substrates⁷ of type **1** have been used. The pa-inserted products of type **2** are already known.¹ The reaction of ha with **1** proceeds smoothly in CH_2Cl_2 –MeOH mixtures under mild conditions, affording the type **3** species in virtually quantitative yield. To our knowledge, this reaction represents the first authentic example of insertion of ha into the Ru–C bond.

Characterization of $\text{Ru}(\text{RL}^3)(\text{PPh}_3)_2(\text{CO})\text{Cl}$, **3.** Spectral and other physical features of **3** are listed in the Experimental Section. The N⁺–H and C=N stretches occur at ~ 3440 and ~ 1620 cm^{-1} , respectively, consistent with the zwitterionic iminium–phenolato function. In ¹H NMR, the N⁺–H and O–H signals occur near δ 12.0 and δ 2.3, respectively (both signals disappear upon shaking with D₂O). The σ -vinyl 10-H proton occurs near δ 6.3 as a singlet.

The structure of **3a** has been determined (Figure 2, Table 1). In the distorted octahedral coordination sphere, the nearly linear P–Ru–P axis lies approximately perpendicular to the plane (mean deviation of 0.02 Å) of the RuC₂ClO meridian. The hydroxymethyl group is tilted away from the meridian and lies closer to P2 than P1, their distances from the O3 atom being 5.176(16)

(7) Ghosh, P.; Bag, N.; Chakravorty, A. *Organometallics* **1996**, *15*, 3042. (b) Bag, N.; Choudhury, S. B.; Pramanik, A.; Lahiri, G. K.; Chakravorty, A. *Inorg. Chem.* **1990**, *29*, 5013. (c) Bag, N.; Choudhury, S. B.; Lahiri, G. K.; Chakravorty, A. *J. Chem. Soc., Chem. Commun.* **1990**, 1626.

(1) Ghosh, K.; Pattanayak, S.; Chakravorty, A. *Organometallics* **1998**, *17*, 1956 and references therein.

(2) Bruce, M. I.; Catlaw, A.; Cifuentes, M. P.; Snow, M. R.; Tiekink, E. R. T. *J. Organomet. Chem.* **1990**, *397*, 187.

(3) Lutsenko, Z. L.; Aleksandrov, G. G.; Petrovskii, P. V.; Shubina, E. S.; Andrianov, V. G.; Struchkov, Yu. T.; Rubezhov, A. Z. *J. Organomet. Chem.* **1985**, *281*, 349.

(4) Garn, D.; Knoch, F.; Kish, H. *J. Organomet. Chem.* **1993**, *444*, 155.

(5) Barns, R. M.; Hubbard, J. L. *J. Am. Chem. Soc.* **1994**, *116*, 9514.

(6) Ferstl, W.; Sakodinskaya, I. K.; Beydoun-Sutter, N.; Borgne, G. L.; Pfeffer, M.; Ryabov, A. D. *Organometallics* **1997**, *16*, 411.

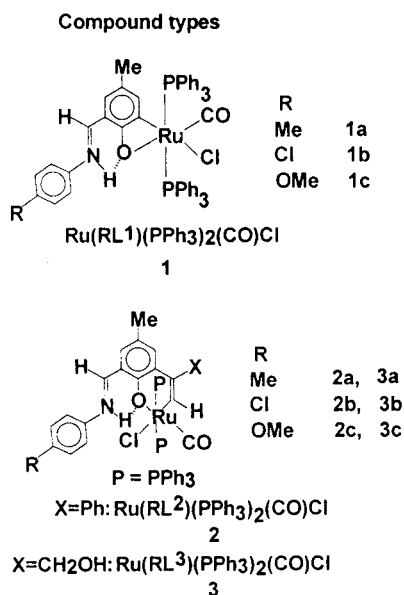


Figure 1. Substrates and alkyne-inserted organometallics of this work.

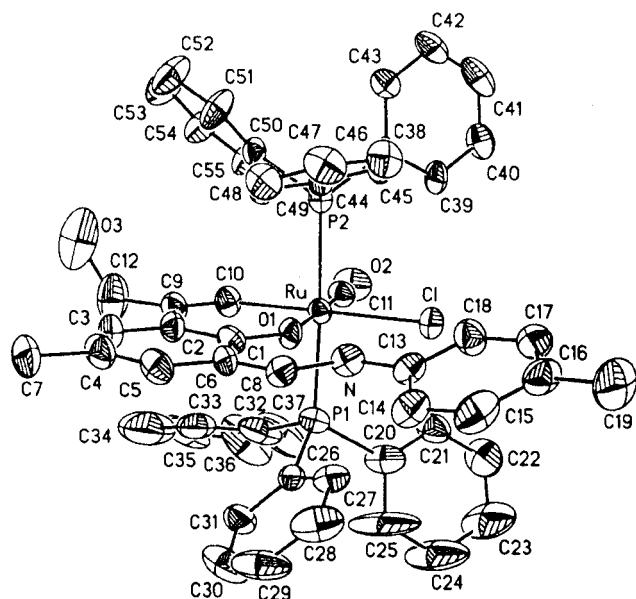


Figure 2. ORTEP plot (30% probability ellipsoids) and atom-labeling scheme for **3a**.

and 6.275(18) Å, respectively. The chelate ring is nearly planar (mean deviation of 0.02 Å), and indeed, the RuRL³ fragment excluding MeC₆H₅, Me, and CH₂OH groups is approximately planar (mean deviation of 0.04 Å). The Ru–C10 (sp²) bond is ~0.2 Å longer than Ru–C11 (sp) bond. The Ru–Cl bond is longer than usual because of the trans influence of the σ -vinyl site as observed previously.¹

Insertion Rates. These have been determined spectrophotometrically in CH₂Cl₂–MeOH mixtures over a range of temperature. The two reactions studied in detail are stated in eq 2. The spectra of the reacting



solutions (Figure 3, case of ha) are characterized by multiple isosbestic points, strongly implicating⁹ that **1a** and the expanded metallacycle are the only stable absorbing species. Studies in 2:1 CH₂Cl₂–MeOH mix-

Table 1. Selected Bond Lengths [Å] and Angles [deg] for Ru(RL³)(PPh₃)₂(CO)Cl, **3A**

Distances			
Ru–C(11)	1.820(13)	Ru–Cl	2.530(3)
Ru–C(10)	2.020(11)	O(1)–C(1)	1.284(13)
Ru–O(1)	2.100(7)	O(2)–C(11)	1.153(13)
Ru–P(1)	2.365(4)	N–C(8)	1.325(14)
Ru–P(2)	2.376(3)	C(9)–C(10)	1.363(16)
N···O(1)	2.608(12)		
Angles			
C(11)–Ru–C(10)	91.4(5)	P(1)–Ru–P(2)	177.26(12)
C(11)–Ru–O(1)	178.1(4)	C(11)–Ru–Cl	99.6(4)
C(10)–Ru–O(1)	86.9(4)	C(10)–Ru–Cl	168.8(4)
C(11)–Ru–P(1)	89.2(4)	O(1)–Ru–Cl	82.2(2)
C(10)–Ru–P(1)	89.4(3)	P(1)–Ru–Cl	93.08(12)
O(1)–Ru–P(1)	90.0(2)	P(2)–Ru–Cl	89.12(11)
C(11)–Ru–P(2)	92.0(4)	C(1)–O(1)–Ru	131.0(7)
C(10)–Ru–P(2)	88.1(3)	C(9)–C(10)–Ru	129.8(10)
O(1)–Ru–P(2)	88.7(2)	O(2)–C(11)–Ru	177.6(11)

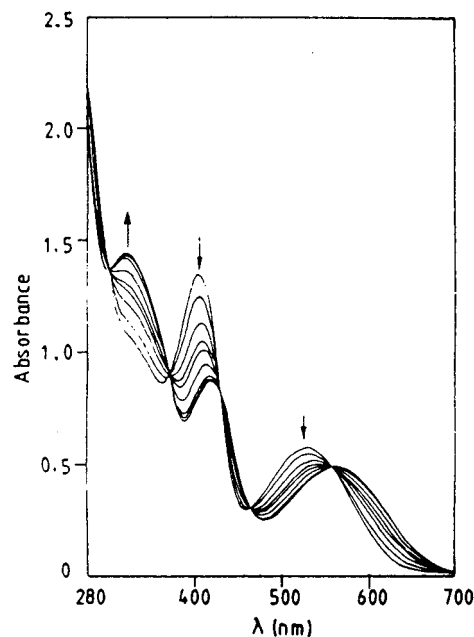


Figure 3. Spectral time evolution in the reaction of **1a** (1.27×10^{-4} M) with ha (9.97×10^{-3} M) in CH₂Cl₂–MeOH (8.14 M in MeOH) solution at 308 K.

tures in the presence of a large excess (>10-fold) of xa over **1a** have revealed the rate law of eq 3, the pseudo-

$$\text{rate} = k_{\text{obs}}[\mathbf{1a}] \quad (3)$$

first-order rate constant k_{obs} being proportional to the concentration of xa. It was further observed that the insertion process failed to proceed in pure CH₂Cl₂. This prompted us to examine the rate as a function of methanol concentration at constant xa concentration. The rate was found to be proportional to the concentration of methanol. The consolidated concentration dependence of k_{obs} is stated in eq 4 where K_{xa} is a constant, vide infra.

$$k_{\text{obs}} = K_{\text{xa}}[\text{xa}][\text{MeOH}] \quad (4)$$

(8) Chevalier, P.; Sandorfy, C. *Can. J. Chem.* **1960**, *38*, 2524. (b) Bohme, H.; Haake, M. In *Advances in Organic Chemistry*; Bohme, H., Vieche, H. G., Eds.; Interscience: New York, 1976; Part 1, Vol. 9, p 1. (c) Farvot, J.; Vocelle, D.; Sandorfy, C. *Photochem. Photobiol.* **1979**, *30*, 417. (d) Sandorfy, C.; Vocelle, D. *Mol. Phys. Chem. Biol.* **1989**, *4*, 195.

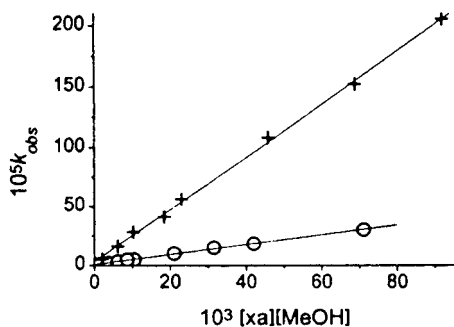


Figure 4. Plots of k_{obs} vs $[xa][\text{MeOH}]$ at 313 K: (+) ha; (o) pa.

Table 2. Rate Data for Reaction of 1a and pa in CH_2Cl_2 -MeOH Mixture

T , K	$10^4[1a]$, M	$10^3[pa]$, M	$10^3[pa][\text{MeOH}]$, M^2	$10^5 k_{\text{obs}}$, s^{-1} ^a	$10^3 k_{\text{pa}} K$, $\text{s}^{-1} \text{M}^{-2}$	
308	1.11	1.32	10.74	3.3(1)	2.6(4)	
		2.64	21.49	5.6(4)		
		3.96	32.23	7.4(2)		
		5.28	42.98	11.9(1)		
313	1.19	1.29	10.50	4.9(2)	4.2(1)	
		2.58	21.00	9.9(1)		
		3.87	31.50	14.8(3)		
		5.16	42.00	18.2(3)		
318	1.10	0.50	1.23	0.9(1)	6.0(5)	
		1.38	9.61	3.70		1.9(3)
		1.10	1.32	6.17		3.3(2)
		2.64	21.49	8.64		4.8(4)
323	1.27	1.29	10.50	9.6(1)	7.1(1)	
		2.58	21.00	17.0(3)		
		3.87	31.50	24.0(1)		
		5.16	42.00	32.0(2)		

^a Least-squares deviations are given in parentheses.

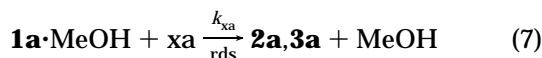
The plots of observed rate constants vs $[xa][\text{MeOH}]$ encompassing large variations in the concentrations of xa and MeOH are excellently (correlation factor of 0.99) linear (Figure 4). Rate data are listed in Tables 2 (for pa) and 3 (for ha).

Methanol Adduct. The relation of eq 4 is consistent with the presence of a methanol adduct occurring in equilibrium, the equilibrium constant being K , eqs 5 and 6. The methanol adduct is taken as the reactive inter-



$$K = \frac{[1a \cdot \text{MeOH}]}{[1a][\text{MeOH}]} \quad (6)$$

mediate as in eq 7, which is the rate-determining step



(rds). The corresponding rate law given in eq 8 is characterized by the rate constant k_{xa} . The relation of

$$\text{rate} = k_{\text{xa}}[1a \cdot \text{MeOH}][xa] \quad (8)$$

Table 3. Rate Data for Reaction of 1a and ha in CH_2Cl_2 -MeOH Mixture

T , K	$10^4[1a]$, M	$10^3[ha]$, M	$10^3[ha][\text{MeOH}]$, M^2	$10^5 k_{\text{obs}}$, s^{-1} ^a	$10^3 k_{\text{ha}} K$, $\text{s}^{-1} \text{M}^{-2}$
298	1.79	2.82	22.95	23.0(4)	7.2(4)
		5.64	45.90	43.0(3)	
		8.46	68.86	56.0(2)	
		11.28	91.82	74.0(3)	
303	1.83	2.92	23.77	24.0(3)	11.1(4)
		5.84	47.54	52.0(2)	
		8.76	71.31	77.0(3)	
		11.28	91.82	108.0(4)	
308	1.83	2.92	23.77	35.0(1)	13.2(1)
		5.84	47.54	67.0(3)	
		8.76	71.31	98.0(4)	
		11.28	91.82	205.0(4)	
313	1.79	2.82	22.95	56.0(3)	22.0(3)
		5.64	45.90	108.0(4)	
		8.46	68.86	152.0(2)	
		11.28	91.82	205.0(4)	
	0.49	0.83	2.04	5.2(2)	
			6.14	16.0(3)	
			10.24	28.0(1)	
			18.43	41.0(3)	

^a Least-squares deviations are given in parentheses.

eq 4 is readily derived by combining eqs 3, 6, and 8, the constant K_{xa} of eq 4 being related to K and k_{xa} as in eq 9.

$$K_{\text{xa}} = K k_{\text{xa}} \quad (9)$$

The value of K_{xa} increases with increasing temperature (Tables 2 and 3), and the Eyring equation is obeyed. The corresponding activation enthalpies (ΔH^\ddagger) are 12.9-(1.0) and 12.5(1.0) kcal mol⁻¹ and the activation entropies (ΔS^\ddagger) are -28.9(2.9) and -26.7(2.7) eu, respectively, for the pa and ha insertions. The rate-determining step is thus associative in nature. We have not succeeded, however, in determining k_{xa} and K separately, and both quantities are expected to be temperature-dependent. This has vitiated estimation of true activation parameters, which must relate only to k_{xa} . It is possible, however, to estimate genuine relative rate constants for the pa and ha reactions with a given type 1 substrate by virtue of eq 10, which follows from eq 9. Scrutiny of

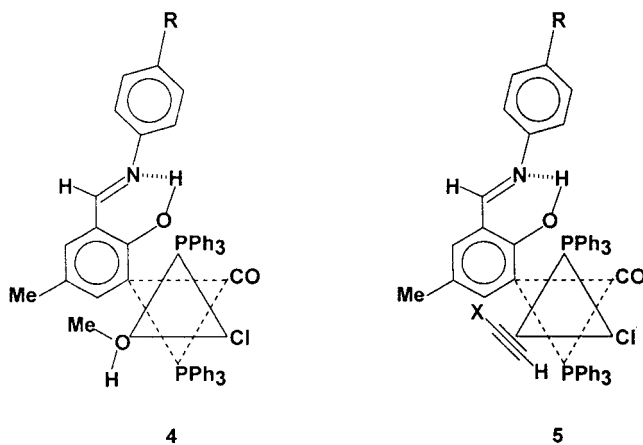
$$\frac{K'_{\text{ha}}}{K'_{\text{pa}}} = \frac{k_{\text{ha}}}{k_{\text{pa}}} \quad (10)$$

Table 2 reveals that at a given temperature $k_{\text{ha}} \approx 5k_{\text{pa}}$. This is qualitatively reflected in the much higher slope of the ha line in Figure 4.

Reaction Model. Solutions of 1a in CH_2Cl_2 -MeOH are nonconducting, and the insertion rate is not affected by the presence of even large excess of (>10-fold) chloride ($\text{Et}_4\text{NCl/LiCl}$) and PPh_3 in the reaction medium. These observations militate against possible displacement of chloride and phosphine ligands by methanol. On the other hand, the Ru-O(phenolato) bond in type 1 species is relatively weak and is known to be readily displaced by Lewis bases.¹⁰ It is proposed that methanol acts as a Lewis base, generating the reactive adduct stylized as 4. Alkyne π -anchoring and activation is believed to occur via displacement of methanol as in 5. Rapid 2 + 2 addition between C \equiv C and Ru-C (aryl) and reestablishment of the Ru-

(9) Wilkins, R. G. *Kinetics and Mechanism of Reactions of Transition Metal Complexes*, 2nd ed.; VCH: New York, 1991; p 156.

(10) Ghosh, P.; Pramanik, A.; Chakravorty, A. *Organometallics* **1996**, *15*, 4147. (b) Ghosh, P.; Chakravorty, A. *Inorg. Chem.* **1997**, *36*, 64.



O(phenolato) bond complete the metallacycle expansion, affording **2** or **3**.

Space-filling models reveal that the 2 + 2 addition reaction is subject to steric crowding¹ from Cl and PPh₃ ligands, and this can explain the regioselectivity of the insertion reaction characterized by the addition of ≡CX and ≡CH fragments, respectively, to the carbon and metal ends of Ru–C bond.

To our knowledge, the only other reported kinetic study of alkyne insertion into Ru–C bond concerns certain orthoruthenated *N,N*-dimethylbenzylamine species⁶ wherein, unlike in our system, the reaction involves displacement of chloride by methanol.

Effect of Substituents. The 2 + 2 addition process involves nucleophilic attack on the metal. Electron withdrawal from metal via the Schiff base ligand should therefore make insertion more facile. The k_{obs} (Table 4) values for all three type **1** species were determined for both pa and ha under invariant conditions of temperature (40 °C) and concentrations (alkyne and MeOH). The R substituents are found to affect k_{obs} significantly, and it increased with increasing electron withdrawal: OMe < Me < Cl. Indeed, the plots of log k_{obs} vs Hammett constants¹¹ of R are found to be linear for both pa and ha insertions.

Electron-rich alkynes would be expected to insert more quickly, as ha does compared to pa. The smaller steric bulk of CH₂OH compared to Ph is also an advantage of ha over pa. The net observed effect is that ha reacts 5 times faster than pa.

Concluding Remarks

The main finding of this work will now be summarized. The insertion of ha into **1** has afforded the expanded metallacycle **3** in nearly quantitative yields. Rate studies in the cases of pa and ha in CH₂Cl₂–MeOH mixtures have revealed that the reactive intermediate is the methanol adduct **1**·MeOH presumably belonging to structural type **4**. The latter anchors and activates the alkyne via displacement of MeOH as in **5**. Sterically controlled regioselective 2 + 2 addition between C≡C and Ru–C (aryl) bonds follows, finally affording **2** and **3**.

Electronic and steric features make ha 5 times more reactive than pa. The R substituents affect the reactivity

Table 4. Observed Rate Constants for the Insertion of pa and ha into Ru(RL¹)(PPh₃)₂(CO)Cl for Different R at 313 K in CH₂Cl₂–MeOH Mixture^a

R	pa insertion			ha insertion		
	10 ⁴ [1a], M	10 ⁴ [pa], M	10 ³ k_{obs} , min ⁻¹	10 ⁴ [1a], M	10 ⁴ [ha], M	10 ³ k_{obs} , min ⁻¹
Me	0.15		4.1(1)	0.45		14.3(1)
Cl	0.15	4.68	8.6(1)	0.43	9.20	24.7(3)
OMe	0.17		3.8(1)	0.44		12.2(1)

^a [MeOH] = 22.21 M.

of **1**, the rate increasing with increasing electron withdrawal (OMe < Me < Cl).

Experimental Section

Materials. The compounds Ru(PPh₃)₃Cl₂¹² and Ru(RL¹)(PPh₃)₂(CO)Cl⁷ were prepared as reported. Phenylacetylene and hydroxymethylacetylene (propargyl alcohol) were obtained from Aldrich. The purification of dichloromethane and methanol was done as described before.¹³ All other chemicals and solvents were of analytical grade and were used as received.

Physical Measurements. Electronic and IR spectra were recorded with a Shimadzu UV-1601PC spectrophotometer (thermostated cell compartment) and Perkin-Elmer 783 IR spectrophotometer. ¹H NMR spectra were obtained using a Bruker 300 MHz FT NMR spectrophotometer (tetramethylsilane internal standard). Microanalyses (C, H, N) were done by using a Perkin-Elmer 240 C elemental analyzer. Solution electrical conductivity was measured by a Philips PR 9500 bridge using a platinized conductivity cell with a cell constant of 1.0.

Preparation of Complexes. Ru(RL³)(PPh₃)₂(CO)Cl complexes were synthesized in nearly quantitative (~98%) yield by reacting Ru(RL¹)(PPh₃)₂(CO)Cl in a CH₂Cl₂–MeOH mixture with excess ha. Details of a representative case are given below. The other compounds were prepared analogously.

[Ru(MeL³)(PPh₃)₂(CO)Cl] (3a**).** In a round-bottom flask Ru(MeL¹)(PPh₃)₂(CO)Cl (50 mg, 0.054 mmol) was dissolved in a 2:1 (by volume) CH₂Cl₂–MeOH mixture and ha (30 mg, 0.536 mmol) was added to it. The mixture was stirred at 40 °C for 15 min on a magnetic stirrer. The color of the solution changed from violet to green. When the solution was concentrated and cooled, a green crystalline solid separated, which was collected, washed thoroughly with methanol, and dried in vacuo. Yield, 52 mg (98%); mp, 152 °C. Anal. Calcd for RuC₅₅H₄₈NO₃P₂Cl: C, 68.14; H, 4.99; N, 1.44. Found: C, 68.19; H, 4.91; N, 1.46. ¹H NMR (CDCl₃, δ): 6.44 (s, 1H arom), 6.34 (s, 1H, C=CH(Ru)), 3.71–3.79 (m, 2H, –CH₂–), 2.29 (s, 1H, OH), 12.72 (m, 1H, =N⁺H), 7.04–7.92 (m, 35 H, arom and –HC=N⁺), 2.12 (s, 3H, –CH₃), 2.29 (s, 3H, –CH₃). IR (KBr, cm⁻¹): ν(C=N) 1620; ν(C=O) 1900; ν(N–H, hexachlorobutadiene) 3440. UV–vis (CH₂Cl₂, λ_{max}, nm (ε, M⁻¹ cm⁻¹)): 575 (2600), 420 (5070), 320 (8050).

[Ru(CiL³)(PPh₃)₂(CO)Cl] (3b**).** Yield, 51 mg (96%); mp, 155 °C. Anal. Calcd for RuC₅₄H₄₅NO₃P₂Cl₂: C, 65.52; H, 4.58; N, 1.42. Found: C, 65.57; H, 4.53; N, 1.45. ¹H NMR (CDCl₃, δ): 6.43 (s, 1H arom), 6.33 (s, 1H, C=CH(Ru)), 3.71–3.79 (m, 2H, –CH₂–), 2.31 (s, 1H, OH), 12.66 (m, 1H, =N⁺H), 7.11–7.96 (m, 35 H, arom and –HC=N⁺), 2.11 (s, 3H, –CH₃). IR (KBr, cm⁻¹): ν(C=N) 1610; ν(C=O) 1890; ν(N–H, hexachlorobutadiene) 3440. UV–vis (CH₂Cl₂, λ_{max}, nm (ε, M⁻¹ cm⁻¹)): 570 (4650), 420 (8850), 320 (14400).

[Ru(MeOL³)(PPh₃)₂(CO)Cl] (3c**).** Yield, 52 mg (98%); mp, 153 °C. Anal. Calcd for RuC₅₅H₄₈NO₄P₂Cl: C, 67.04; H, 4.91; N, 1.42. Found: C, 67.01; H, 4.88; N, 1.43. ¹H NMR (CDCl₃,

(12) Stephenson, T. A.; Wilkinson, G. J. *Inorg. Nucl. Chem.* **1966**, *28*, 945.

(13) Vogel, A. I. *Practical Organic Chemistry*, 3rd ed.; ELBS and Longman Group: Harlow, England, 1965; pp 176, 169.

(11) Finar, I. L. *Organic Chemistry, Vol. 1: Fundamental Principles*, 6th ed.; ELBS, Longman Group: Essex, England, 1990; p 605.

δ): 6.44 (s, 1H arom), 6.34 (s, 1H, C=CH(Ru)), 3.71–3.76 (m, 5H, –CH₂– and –OMe), 2.31 (s, 1H, OH), 12.71 (m, 1H, =N⁺H), 7.13–7.90 (m, 35H, arom and –HC=N⁺), 2.12 (s, 3H, –CH₃). IR (KBr, cm⁻¹): ν (C=N) 1610; ν (C=O) 1890; ν (N–H, hexachlorobutadiene) 3440. UV–vis (CH₂Cl₂, λ_{\max} , nm(ϵ , M⁻¹ cm⁻¹)): 570 (2460), 420 (4510), 320 (9120).

Rate Measurements. Measurements were carried out in CH₂Cl₂–MeOH mixtures by observing the change in absorbances at 403 nm for pa and at 408 nm for ha. The k_{obs} values were calculated from a linear plot of $-\ln(A_t - A_\infty)$ vs t , where A_t and A_∞ are the absorbances at time t and at the end of reaction (48 h), respectively. The activation enthalpy (ΔH^\ddagger) and entropy (ΔS^\ddagger) were calculated from the variable-temperature rate constant, using the Eyring equation, eq 11 (k_B and h are the Boltzmann constant and Planck's constant, respectively).

$$k = \frac{k_B T}{h} \left[\exp\left(\frac{-\Delta H^\ddagger}{RT}\right) \exp\left(\frac{\Delta S^\ddagger}{R}\right) \right] \quad (11)$$

The plots of $-\ln[k_{\text{obs}} h / (k_B T)]$ vs $1/T$ were satisfactorily linear (correlation factor of 0.98). The curve fit and all other calculations were done with the Microcal Origin, version 4.0, software package.

X-ray Structure Determination. Single crystals of Ru(MeL³)(PPh₃)₂(CO)Cl, **3a** (0.25 × 0.25 × 0.40 mm³) were grown (at 298 K) by slow diffusion of hexane into dichloromethane solution followed by evaporation. The crystals were inherently poor in quality, giving rise to broadened diffraction peaks, and only moderately good refinement could be achieved. The thermal parameters are relatively high, especially for one phenyl ring on the P1 atom. Cell parameters were determined by a least-squares fit of 30 machine-centered reflections ($2\theta = 15$ – 30°). Data were collected with the ω -scan technique in the range $3^\circ \leq 2\theta \leq 45^\circ$ on a Siemens R3m/V four-circle diffractometer with graphite-monochromated Mo K α radiation ($\lambda = 0.71073 \text{ \AA}$). Two check reflections measured after every 198 reflections showed no significant intensity reduction in any case. All data were corrected for Lorentz polarization

(14) North, A. C. T.; Phillips, D. C.; Mathews, F. A. *Acta Crystallogr., Sect. A* **1968**, *24*, 351.

(15) Sheldrick, G. M. *SHELXTL*, version 5.03; Bruker Analytical X-ray Systems: Madison, WI, 1994.

Table 5. Crystal, Data Collection, and Refinement Parameters for Ru(ML³)(PPh₃)₂(CO)Cl, **3a**

mol formula	C ₅₅ H ₄₈ ClNO ₃ P ₂ Ru
mol wt	969.40
cryst syst	monoclinic
space group	<i>P2</i> ₁ / <i>c</i>
<i>a</i> , Å	14.655(8)
<i>b</i> , Å	15.091(6)
<i>c</i> , Å	21.949(14)
β , deg	92.93(5)
<i>V</i> , Å ³	4848(5)
<i>Z</i>	4
λ , Å	0.71073
μ , cm ⁻¹	4.88
<i>D</i> _{calcd} , g cm ⁻³	1.328
<i>R</i> ^a , w <i>R</i> ² ^b [<i>I</i> > 2 σ (<i>I</i>)]	7.95, 18.19

$$^a R = \sum |F_o| - |F_c| / \sum |F_o|. \quad ^b wR2 = [\sum w(F_o^2 - F_c^2)^2 / \sum (F_o^2)^2]^{1/2}.$$

effects, and an empirical absorption correction¹⁴ was done on the basis of an azimuthal scan of six reflections for the crystal.

The metal atom was located from Patterson maps, and the rest of the non-hydrogen atoms emerged from successive Fourier syntheses. The structures were refined by a full-matrix least-squares procedure on *F*². All non-hydrogen atoms were refined anisotropically. Hydrogen atoms were included at calculated positions. Calculations were performed using the SHELXTL, version 5.03,¹⁵ program package. Significant crystal data are listed in Table 5.

Acknowledgment. We thank the Department of Science and Technology, Indian National Science Academy and the Council of Scientific and Industrial Research, New Delhi, for financial support. Affiliation with Jawaharlal Nehru Centre for Advanced Scientific Research, Bangalore, India, is acknowledged. We are thankful to Prof. P. Banerjee for helpful discussions.

Supporting Information Available: X-ray crystallography files, in CIF format, for the structure determination of **3a**. This material is available free of charge via the Internet at <http://pubs.acs.org>.

OM000649C